TOPICAL REVIEW

A review on optical imaging of DNA nanostructures and dynamic processes

To cite this article: Yancheng Du et al 2019 Methods Appl. Fluoresc. 7 012002

View the <u>article online</u> for updates and enhancements.



Methods and Applications in Fluorescence



RECEIVED 23 December 2017

REVISED

11 October 2018

ACCEPTED FOR PUBLICATION 31 October 2018

PUBLISHED 11 January 2019

TOPICAL REVIEW

A review on optical imaging of DNA nanostructures and dynamic processes

Yancheng Du, Jing Pan and Jong Hyun Choi

School of Mechanical Engineering, Purdue University, West Lafayette, IN 47907

E-mail: jchoi@purdue.edu

Keywords: DNA nanotechnology, self-assembly, fluorescence, super-resolution microscopy

Abstract

DNA self-assembly offers a powerful means to construct complex nanostructures and program dynamic molecular processes such as strand displacement. DNA nanosystems pack high structural complexity in a small scale (typically, <100 nm) and span dynamic features over long periods of time, which bring new challenges for characterizations. The spatial and temporal features of DNA nanosystems require novel experimental methods capable of high resolution imaging over long time periods. This article reviews recent advances in optical imaging methods for characterizing self-assembled DNA nanosystems, with particular emphasis on super-resolved fluorescence microscopy. Several advanced strategies are developed to obtain accurate and detailed images of intricate DNA nanogeometries and to perform precise tracking of molecular motions in dynamic processes. We present state-of-the-art instruments and imaging strategies including localization microscopy and spectral imaging. We discuss how they are used in biological studies and biomedical applications, and also provide current challenges and future outlook. Overall, this review serves as a practical guide in optical microscopy for the field of DNA nanotechnology.

1. Introduction

Over the several decades since the discovery of DNA double helix [1], significant efforts have been devoted to understanding the biochemical and biophysical properties of DNA [2–4]. A DNA strand consists of four distinct bases, adenine (A), thymine (T), guanine (G), and cytosine (C), in a specific order along the sugar-phosphate backbone. The complementarity between A and T and G and C via hydrogen bonds not only carries genetic information, but also offers a powerful strategy for molecular self-assembly. In 1982, Seeman first proposed to construct a holiday junction by connecting 4 strands, each of which has a single-stranded overhang that is complementary to one another [5]. This simple concept was adopted by numerous research groups and has now grown into the field of DNA nanotechnology [6]. Along the progress in DNA self-assembly, the synthesis of oligonucleotides becomes more efficient, thus the price has decreased drastically over the past two decades (~\$0.10 per base) [7–9]. DNA chemistry also has advanced such that various chemical moieties such

as fluorophores, affinity ligands, radioactive elements, proteins and enzymes may be engineered onto oligonucleotides, and there is a library of modified DNA strands commercially available. These advances together make DNA as powerful engineering tools for widespread applications including biochemical sensors, materials synthesis/placement, biophysical tools, drug/payload delivery, nanomechanical systems, molecular computations, and synthetic biology [6, 10–22].

There are several distinct strategies for designing and constructing complex nanoscale materials from DNA. These strategies may be classified as two kinds [23]. One is building structures from small motifs; these strands can have certain geometric patterns and bind with each other, forming complex geometries or large matrices. Tile-based assembly and DNA bricks follow such principles. The other strategy is DNA origami, a widely popular method for constructing nanoscale structures and patterns from in silico designs. DNA origami uses a long single strand of DNA (typically genome of M13 bacteriophage) as a scaffold which is folded in a predesigned pattern with

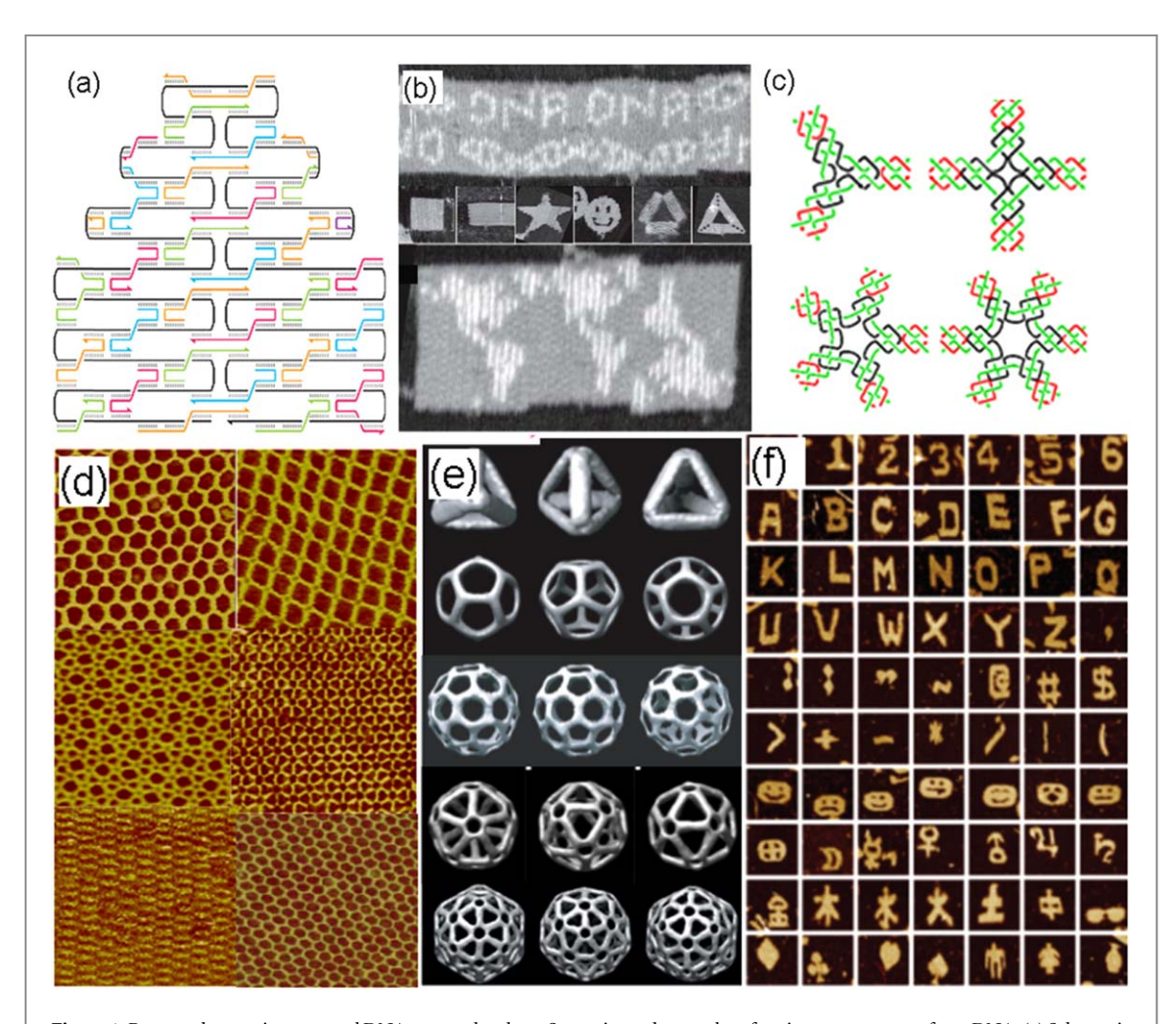


Figure 1. Recent advances in structural DNA nanotechnology. Strategies and examples of static nanostructures from DNA. (a) Schematic of DNA origami method. A long genomic DNA scaffold (black line) is folded into a predesigned pattern by short staple strands (shown in blue, green, orange, and magenta). Adapted from [24] with permission. Copyright © 2006, Springer Nature. (b) AFM images of DNA origami structures. Adapted from [24] with permission. Copyright © 2006, Springer Nature. (c) Schematics of tile-based approaches. High-symmetry DNA motifs. Adapted in part from [43] with permission. Copyright © 2008, Springer Nature, [44] with permission. © Proceedings of the National Academy of Sciences (2008), [45] with permission. Copyright © 2010, Springer Nature and [49] John Wiley & Sons. © 2014 WILEY-VCH Verlag GmbH & Co. KGaA, Weinheim. (d) AFM images of highly periodic 2D lattices. Adapted in part from [44] with permission. © Proceedings of the National Academy of Sciences (2008), [45] with permission. Copyright © 2010, Springer Nature, with permission from [46]. Copyright (2005) American Chemical Society. (e) Images of DNA polyhedra via tile-based assembly reconstructed from cryo-TEM. Adapted in part from [43] with permission. Copyright © 2008, Springer Nature, [44] with permission. © Proceedings of the National Academy of Sciences (2008), [45] with permission. Copyright © 2010, Springer Nature, [44] with permission. © Proceedings of the National Academy of Sciences (2008), [45] with permission. Copyright © 2010, Springer Nature, [44] with permission. © Proceedings of the National Academy of Sciences (2008), [45] with permission. Copyright © 2010, Springer Nature, [44] with permission. © Proceedings of the National Academy of Sciences (2008), [45] with permission. Copyright © 2010, Springer Nature, [44] with permission. © Proceedings of the National Academy of Sciences (2008), [45] with permission. Copyright © 2010, Springer Nature, [44] with permission. © Proceedings of the National Academy of Sciences (2008), [

the help of a large number of engineered oligonucleotides, so-termed staples (figure 1(a)) [24-27]. This approach is robust and fault-tolerant with high reproducibility, offering a unique way to manufacture arbitrarily-shaped structures with a size of ~100 nm (figure 1(b)) [28-42]. Tile-based assembly uses small nucleic acid motifs with sticky ends to construct target geometries. High-symmetry motifs, such as 3-pointstar and 5-point-star motifs (figure 1(c)), may be arranged to form 2D periodic lattices or 3D structures including tetraheron, dodecahedron, buckyball, and icosahedron (figures 1(d), (e)) [43–48]. A combination of two or more multi-point-star motifs can form the even more complex geometries including pentakis dodecahedra (bottom panel in figure 1(e)) [49]. Finite complex shapes may also be created from a large

number of uniquely addressable tiles, rather than high-symmetry assembly of few motifs. This strategy is called single-stranded tiles (SST) or DNA bricks. Figure 1(f) shows examples of such structures from SST with concatenated sticky ends which binds to four local neighbors during self-assembly [50]. The SST approach can also be extended for fabricating 3D geometries. The SST bricks are designed with sticky ends in different directions such that they self-assemble perpendicularly as well as in parallel direction, thus forming 3D patterns [51]. This method is flexible in that each strand is unique and addressable, and has the ability to create large-scale structures (e.g. up to 1 GDa) [52]. Its drawback, however, is the complexity of the strands which may result in a low yield compared to tile-based assembly.

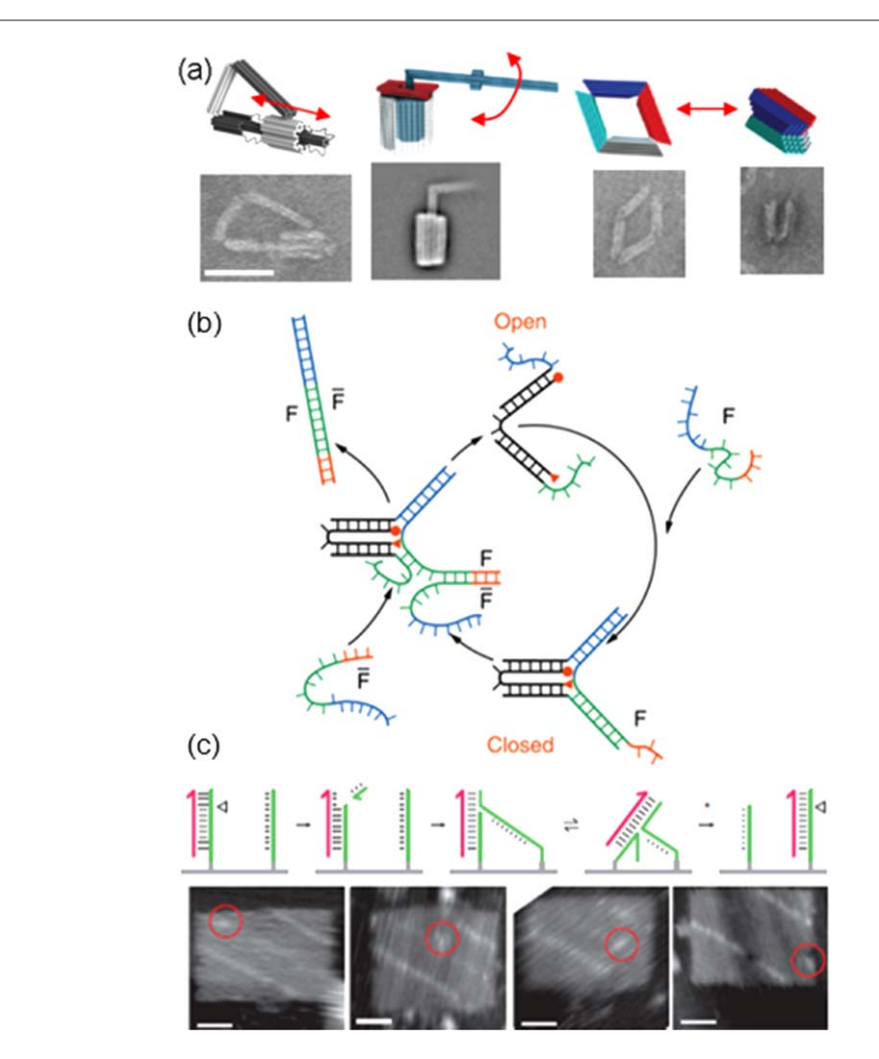


Figure 2. Dynamic DNA structures and processes. (a) Various examples of reconfigurable DNA structures and corresponding TEM images. Adapted from [53] with permission. © Proceedings of the National Academy of Sciences (2015). (b) Schematic of a DNA tweezer with open and close conformations based on toehold-mediated strand displacement. Strand F binds with two arms with single-stranded overhang (shown in red; used as a toehold subsequently) and closes the tweezer. Strand $\overline{\mathbb{F}}$ which is fully complementary to F binds with F and releases it by toehold-mediated strand displacement. The tweezer returns to the open state after the release. Adapted from [56] with permission. Copyright © 2000, Springer Nature. (c) Schematic of a DNA walker that moves along prescriptive landscape and corresponding AFM images. Adapted from [61] with permission. Copyright © 2011, Springer Nature. (The figures are adapted from references cited in the text).

In addition to static structures, DNA self-assembly may also be engineered to program structural reconfigurations and execute dynamic molecular processes or cascade reactions. Figure 2(a) shows several examples of reconfigurable DNA structures [53-55]. These nanomechanical systems are composed of static and dynamic subunits such that dynamic parts can move linearly (e.g. slide back and forth along the track) or rotate in a circle. The relevant shape-changing mechanisms include DNA base-pairing and strand displacement (illustrated in figure 2(b)) [56], thermal activation/cycling [57], biomolecular reactions (e.g. biotin-streptavidin conjugation and protein-aptamer binding) [58, 59], pH changes [60], and electrical/ magnetic fields [55]. Other examples of dynamic DNA systems are switches, tweezers, and motors. In particular, DNA walkers are programmed to move along the prescriptive landscape [61, 62-65], These molecular machines are inspired by intracellular protein

motors such as kinesin and myosin that translocate along microtubules and actin filaments [66–69]. Similar to the biological motors, DNA motors move along the track (e.g. DNA tiles or origami) by converting chemical energy into mechanical motion through a series of conformational changes. In figure 2(c), a DNA walker strand translocates along a predetermined path of foothold strands on an origami tile [61, 65].

The fast developments of DNA nanotechnology demand highly sophisticated characterization tools to image complex nanostructures and probe related mechanical, chemical, and biological properties. Characterization of DNA nanosystems is challenging due to their spatial and temporal features. Static structures typically range from 10 to 100 nm, and consist of highly intricate subunits as shown in figures 1 and 2.[30, 38, 70, 71]. Dynamic processes, driven by strand displacement, enzymatic reactions, or other mechanisms, have a

wide range of temporal characteristics. For example, toe-hold-mediated strand displacement reactions are generally fast (e.g. $\sim 1 \times 10^6$ /s-M), while DNA walkers often suffer from slow kinetics [72, 73]. With a typical walker speed of <1 nm s⁻¹, data/image acquisition may take up to several hours [74–77]. Overall, the characterization of the DNA assemblies and processes must have high spatial and temporal resolution in a wide range.

Traditionally, gel electrophoresis, atomic force microscopy (AFM) [78], and transmission electron microscopy (TEM) [79] have been widely used for DNA characterization, yet they are also limited. For example, gel electrophoresis is a simple and straightforward method that can separate samples based on their molecular weight. However, ensemble samples must be used, and individual molecules or structures cannot be analyzed. AFM can provide precise tomography on the surface in a relatively short time period. AFM uses scanning probes which contact the sample and detect heights or forces. The obtained information may be used to form a topography image of the sample. AFM is a high-resolution method on the order of fractions of a nanometer. However, the AFM tips may perturb DNA structures and this method is not suitable for imaging 3D geometries. TEM uses a beam of electrons passing through the specimen, and the image formed from the interaction between the electrons and the sample can be interpreted to reveal the structure of sample. TEM is powerful in visualizing 3D structures with atomic resolution, yet they are operated under the vacuum or at extremely low temperatures (i.e. cryo-TEM). Staining may be required in biological samples such as DNA for better contrast, and the staining chemicals could affect the integrity of DNA structures. TEM is not suitable for in situ, realtime measurements. Contrary to these non-optical methods, fluorescence imaging has been used in many fields to directly observe structures and motions. It is also applied in DNA nanotechnology. Optical microscopy can address these challenges as a non-invasive imaging platform for fluorescent samples. Recent advances provided novel strategies to overcome the optical diffraction limit which led to the 2014 Nobel Prize in Chemistry and can shed light on DNA structures and functions with high spatial and temporal resolution.

1.1. Subdiffraction Optical microscopy

Traditional optical microscopic methods are limited in imaging individual DNA strands or their assemblies, because of the optical diffraction limit where the spatial resolution is roughly the half of the wavelength or $\sim \lambda/2$ [80, 81]. Several strategies were proposed to overcome the diffraction limit and achieve superresolution images (up to several nanometers) over a long time period (up to several hours) [82–85]. Optical imaging typically uses fluorescent proteins or nucleic

acids functionalized with small organic dyes which emit fluorescence after photo-absorption.

1.1.1. Deterministic methods

Deterministic methods exploit the known absorption and emission spectra of fluorophores or energy transfer between fluorophore pairs to overcome the diffraction limit. One of the most common methods is Förster resonance energy transfer (FRET) that relies on energy transfers between two fluorophores: a donor and an acceptor (figure 3(a)) [86]. The emission energy of the donor is transferred nonradiatively to the acceptor, thus resulting in the decrease of the donor emission and the increase of the acceptor emission. The transfer efficiency is extremely sensitive to the distance between the two fluorophores and follows the equation

$$E = \frac{1}{1 + \left(\frac{r}{R_0}\right)^6}.$$

Therefore, measurement of the FRET efficiency can provide quantitative information about the distance between paired fluorophores with a resolution of under 10 nm [87, 88]. FRET measurement of an ensemble sample exploits strong signals from a large number of molecules, but it is impossible to obtain the information about individual molecules. Therefore, single-molecule FRET or SM-FRET is often used to probe individual molecules and structures.

Another common method is stimulated emission depletion microscopy (STED) which can create superresolution images by selective deactivations of fluorophores. In STED method, a depletion light source is coupled with an excitation source along the same axis (figure 3(b)) [90]. The depletion light deactivates an annulus of fluorophores around the excitation light, thus removing the effects of the unwanted active fluorophores due to the Airy disk formed by the excitation source. The remaining fluorophores significantly improve the image resolution which can achieve ~70 nm [91–93].

1.1.2. Stochastic approaches

Stochastic methods for subdiffraction optical imaging exploit random behaviors of fluorophores that switch between 'on' and 'off' states. At each image acquisition event, only a fraction of fluorophores emits fluorescence which is recorded, while the rest are inactive in the 'off' state. In a series of image acquisitions, the fluorophores become active (i.e. 'on' state) randomly and appear in different image frames. In these images, single fluorophores appear as circular areas with intensity, roughly following Gaussian distribution. These particles are fitted to the distribution functions to estimate the central position of paritcles [89] so that the localization precision is drastically improved [94]. One such strategy is binding activated localization

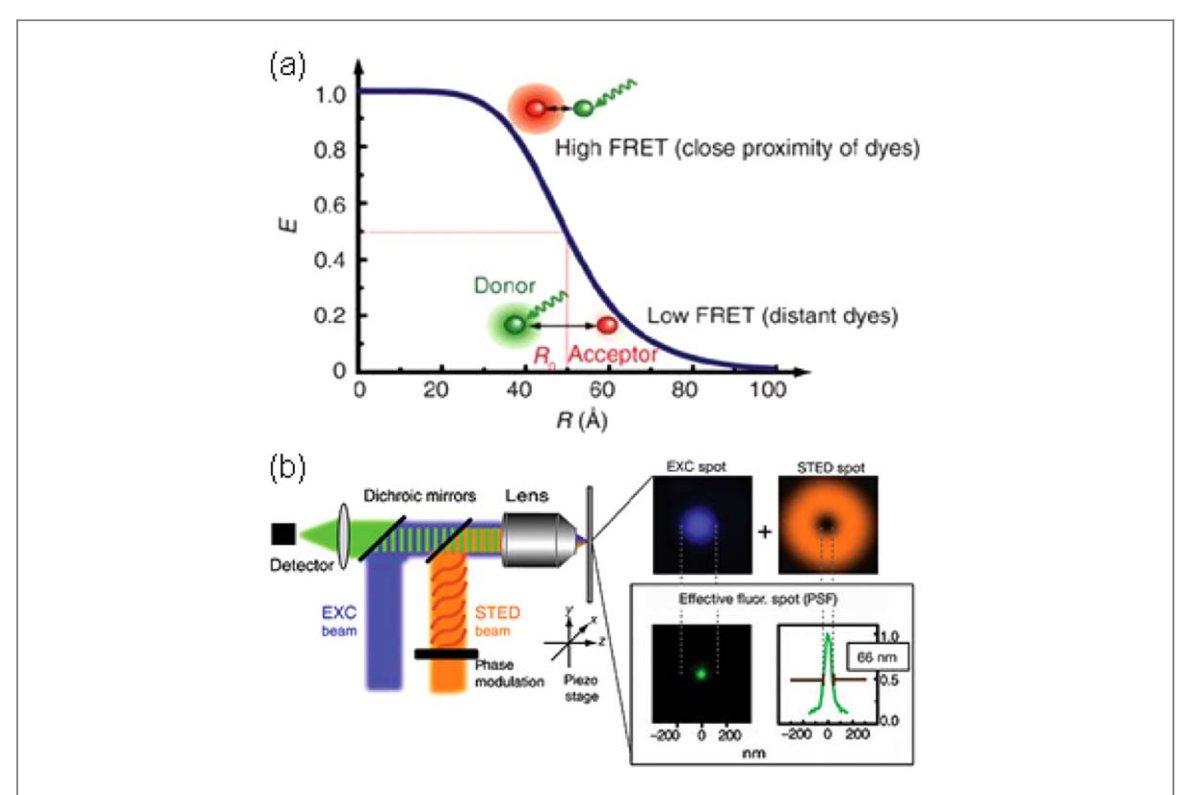


Figure 3. (a) FRET efficiency as a function of the distance between the FRET pair, a donor and an acceptor. When the donor and acceptor are close, the donor will excite the acceptor, yielding high FRET. If the pair is far from each other, they will show low FRET. Adapted from [89] with permission. Copyright © 2008, Springer Nature. (b) Schematic of STED setup. The excitation (EXC) and STED beams are aligned and focused on the same spot, thus resulting in a subdiffraction spot. Adapted from [90] with permission. Copyright © 2006, Springer Nature. (The figures are adapted from references cited in the text).

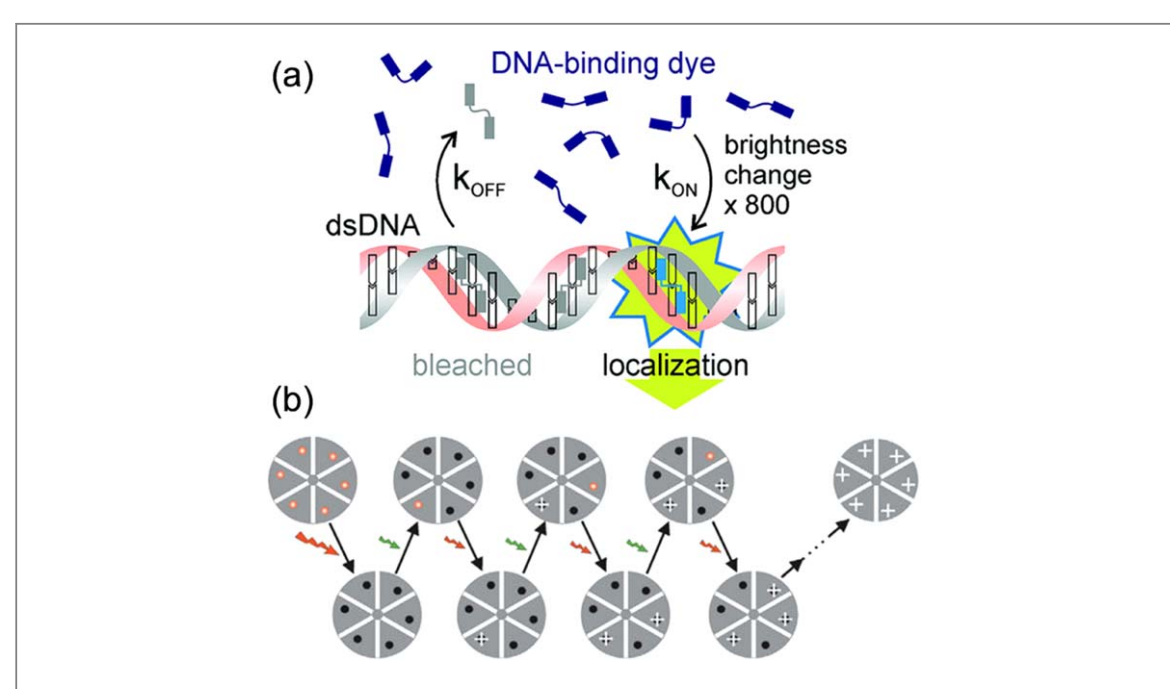


Figure 4. (a) Schematic illustrating the principle of BALM. Adapted from [95] with permission. Copyright © 2016, Springer Nature. Brightness of dyes increase upon binding to target molecules (blue to red), thus enabling measurements and super-resolution images. (b) Principle of STORM using photo-switchable fluorophores to reconstruct super-resolution images. Different fluorophores are excited each acquisition and are combined to form an ensemble image. Adapted from [97] with permission. Copyright © 2006, Springer Nature. (The figures are adapted from references cited in the text).

microscopy or BALM (figure 4(a)) [95]. This method utilizes analyte-binding dyes which reversibly associate with and dissociate from the target structures. The stochastic binding process provides localization

information of the structures with a resolution of approximately 50 nm [94, 96]. Stochastic optical reconstruction microscopy (STORM) is another commonly used method (figure 4(b)). Here, a subset of

photo-switchable fluorophores is activated stochastically at any given moment during imaging. These fluorophores are deactivated at the next acquisition time while another subset is imaged. By iterating this random activation/deactivation process, the fluorophores can be localized and the resulting resolution can achieve ~20 nm [97, 98].

1.1.3. Instrumentation of super-resolution fluorescence microscopy

While the equipment needed for subdiffraction imaging varies with different methods, there are several common featires. For example, total internal reflection fluorescence microscopes (TIRF) [99] are often used, where the entire incident light is internally reflected at the glass-water interface. This forms an evanescent field, which decays exponentially from the interface. Thus, a thin layer of approximately 200 nm is exposed to the incident light. This feature is very useful for observing fluorophores near/on the surface and effectively blocking the fluorophores floating in the solution. As a result, the noise from the floating fluorophores is minimized, thus the signal-to-noise ratio is enhanced. There are mainly two ways to use TIRF: a TIRF objective or a prism. The TIRF objectives have high numerical apertures and easy to use while more expensive. The prisms are low cost, but need to be adjusted in every measurement.

Besides the microscopes, fluorophores, lasers, and detectors are needed. There is a library of fluorophores. For example, Alexa Fluor is a group of fluorescent probes that has a wide range of excitation wavelengths to choose from and are quite stable. Cy3, Cy5 and Cy5.5 are from the cyanine family and widely used in SM-FRET, because the Cy3 emission overlaps well with the excitation spectra of Cy5 and Cy5.5. In biological imaging, green fluorescent proteins (GFP) are often used for labeling in cells and DAPI is used for staining of DNA. The excitation wavelengths of the laser sources depend on the spectral properties of fluorophores used in the measurement. Common laser lines include 488, 543 and 633 nm. Laser power should also be considered, because different fluorophores have a range of quantum yields and they need to be bright enough for measurements and localizations. Lastly, cameras and detectors used for fluorescence imaging need high signal-to-noise ratio. Electron multiplying CCD (EMCCD) or Intensified CCD (ICCD) cameras are widely used, because they can amplify weak signals (i.e. a small number of photons) from single molecules/analytes and provide images of improved quality.

1.2. Scope of this review

This article overviews the state-of-the-art strategies for super-resolution fluorescence imaging of single molecules. Other methods such as AFM and TEM are not discussed as comprehensive reviews may be found elsewhere [100]. In this review, we discuss methods for (1) visualizing static DNA nanostructures including SM-FRET, STED, and BALM and (2) probing dynamic processes such as SM-FRET and single particle tracking (SPT). First, we present several cases of visualizing static DNA nanostructures, with emphasis on how the imaging strategies improve the measurement precision to obtain super-resolved structural information. The latter will highlight how SPT and SM-FRET methods probe dynamic processes, such as monitoring structural changes of DNA and tracking individual fluorophores/particles for kinetic studies. We envision that the case studies will provide practical guides for optical imaging in the field of DNA nanotechnology.

2. Visualizing static DNA nanostructures

The primary methods for visualizing static DNA nanostructures are localization microscopy and SM-FRET. Both approaches are widely used while focusing on different aspects. Localization microscopy provides ensemble information of structures by imaging with high resolution and accuracy. This allows one to directly observe and measure the geometry of individual nanostructures. SM-FRET on the other hand provides indirect structural information (such as distance) by measuring relative intensity of a fluor-ophore pair. This method is mainly used for determining conformation of DNA structures. Below we discuss several examples of these methods.

2.1. Localization microscopy

The development in super-resolution fluorescence microscopy greatly facilitates DNA nanotechnology by providing methods with ultrahigh resolution to allow direct observation of nanostructures. Traditional sub-diffraction strategies such as STED and STORM are widely adopted, while new approaches such as DNA-PAINT also show great potential.

Over the past decade, STED, STORM, and other super-resolution methods are used to greatly improve the imaging resolution. In a previous study, Kim et al used YOYO-1 dye to label stretched DNA fragments (figure 5(a)) [95]. The dye was excited by a 488 nm laser and depleted by a 592 nm laser. They applied the two lasers at the DNA fragments with the STED scheme to greatly reduce the full width half maximum (FWHM) of the signal resolution from 240 to 47 nm. With this method, they performed accurate and precise measurements on lengths of DNA fragments over a wide range. Schoen et al used BALM to acquire high resolution images of DNA structures [96]. The intensities of the fluorescent dyes show significant differences upon binding and unbinding to the DNA sequence. The stochastic binding process between DNA and dyes provide localization information about the DNA molecules and a FWHM of approximately

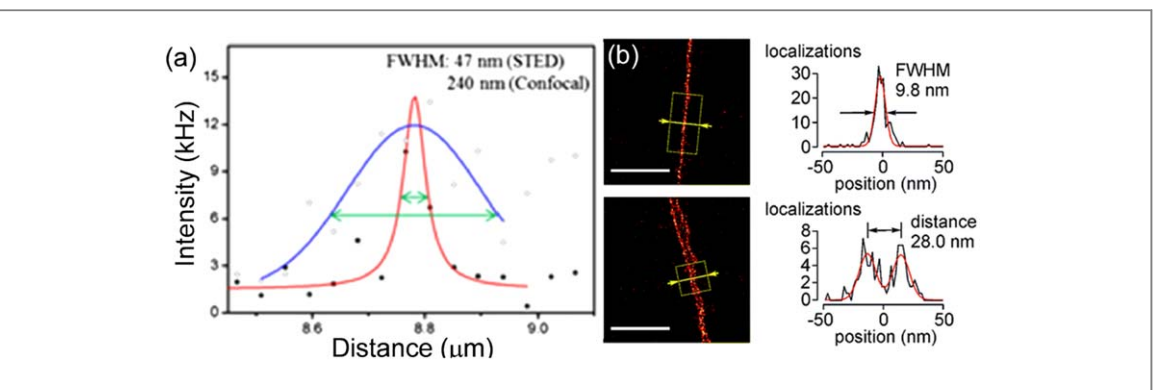


Figure 5. (a) Intensity distributions compares STED and confocal measurements. Adapted from [95] with permission. Copyright © 2016, Springer Nature. The FWHM of STED scheme is \sim 47 nm, whereas traditional confocal microscopy yields \sim 240 nm resolution. (b) Images and corresponding spatial resolution of BALM using DNA-binding dyes, showing a FWHM of \sim 10 nm and distinguishing two DNA fragments distanced by \sim 28 nm. Adapted from [96], Copyright (2011), with permission from Elsevier.

27 nm was demonstrated (figure 5(b)) The development of various super-resolution microscopy schemes requires a wide range of fluorescent dyes to accommodate different spectral characteristics for particular applications.[101–103].

2.1.1. DNA-PAINT

DNA-PAINT, first introduced in 2014 [104], uses programmable and specific binding of dye-labeled DNA probes. These probes are designed to transiently bind to specific locations on DNA nanostructures which makes it photo-switchable and avoids photobleaching. Analysis of the predictable binding kinetics between the probes and the target strands reconstructs super-resolution images. Yin and co-workers used this method to observe various polyhedral structures with different angles and edges, [105]. Each DNA-origami tripod that forms polyhedra carries short docking strands at vertices which are complementary to the dye-labeled DNA probes. Thus, the structure can be imaged with dyes in a controllable way without suffering photobleaching. The DNA-PAINT binding events were localized with a precision of ~5.4 nm in the x-y plane while \sim 9.8 nm in the vertical z direction. They then combined DNA probes with different dyes together to construct fluorescent barcodes. These probes are docked adjacently on DNA origami and create various barcodes by different combinations. The barcodes with sub-micrometer dimensions are shorter than previously reported barcodes and are potentially useful as in situ single-molecule imaging probes for targeting proteins and other biomolecules [106]. As a novel imaging tool, DNA-PAINT can overcome the photobleaching issues in conventional localization microscopy. It also has advantages in controllability and programmability. Yet, there are several challenges to be addressed, including the nonfluorogenic imager strand which may generate a background noise, slow acquisition time, and in vivo imaging.

2.2. SM-FRET

SM-FRET exploits the high sensitivity of paired fluorophores, thus can measure their separation distance at a lengthscale of 1 to 10 nm. This method is commonly used in identifying molecular conformations thanks to the high sensitivity to the distance change within a single molecule. Ha group developed SM-FRET to detect the conformation of a DNA holiday junction, switching between paralleled and perpendicular states (figure 6(a)) [107]. The donor and acceptor fluorophores were attached to two ends of the four-way structure. A low FRET state was monitored when the two ends were separate from each other; a high FRET state was recorded when they were in close proximity. The FRET measurements revealed that the four-way DNA junction intrinsically adopts antiparallel stacked X-conformation. Shirude et al used a similar strategy for an analysis of a G-quadruplex formation [108]. When a G-quadruplex forms, the donor and acceptor are in close proximity, resulting in high FRET signals (figure 6(b)). This study showed that SM-FRET is excellent in identifying DNA and investigating molecular mechanisms in DNA topology. SM-FRET may also be used to investigate bends and kinks in DNA structures. Wozniak et al induced kinks in a DNA structure by inserting unpaired sequence and measured the transfer efficiency for various number of base-pairs between the donor and the acceptor [109]. The experimental results were compared with a geometric model to predict the distance successfully. These studies show that SM-FRET can quantitatively determine the distance in DNA and other molecular structures and should be a valuable platform in structural and biophysical studies [110, 111].

3. Probing dynamic processes

Probing dynamic processes differs from visualization of static structures in that it requires both spatial and temporal resolution for hours or even one day. With growing interest in the conformational change of DNA structures and the movement of DNA based

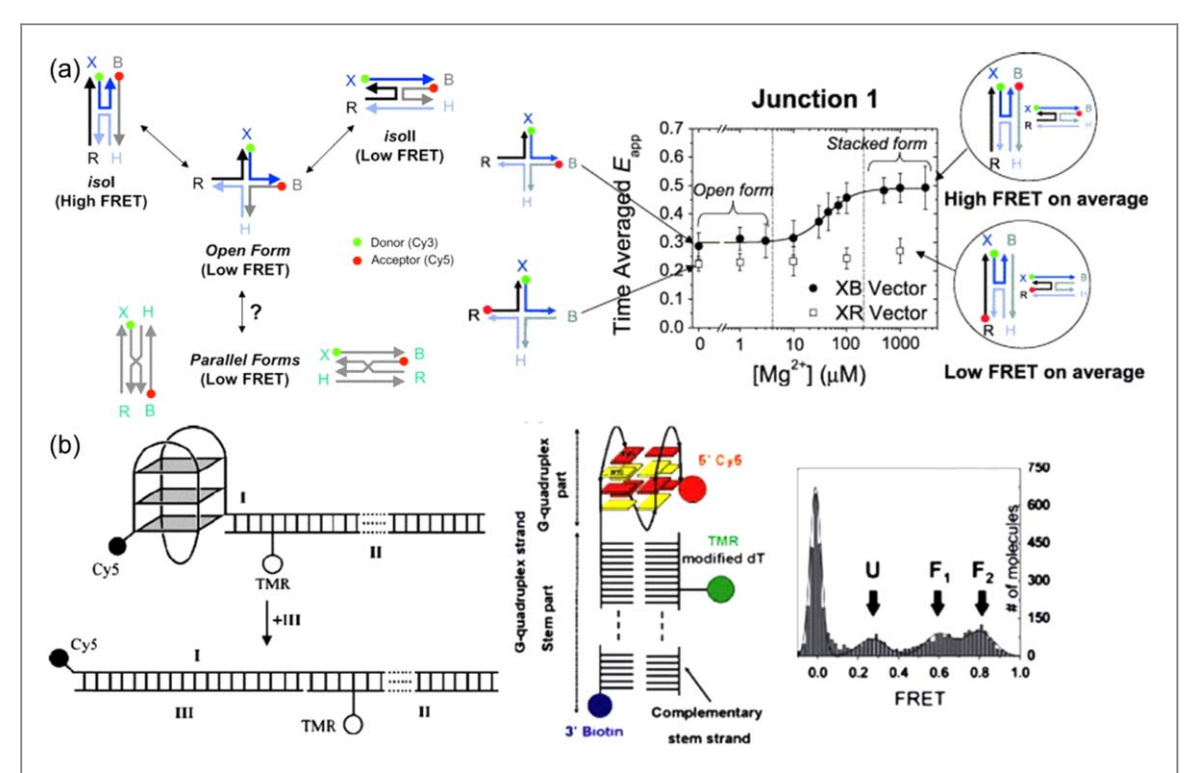


Figure 6. (a) Schematic of open and closed conformations of a DNA holiday junction and corresponding FRET states and efficiency. Adapted from [107], Copyright (2004), with permission from Elsevier. On the left, a pair of donor and acceptor fluorophores are attached to two arms of DNA assembly. The parallel and perpendicular conformations correspond to high and low FRET signals. (b) Folding and unfolding of a G-quadraplex and related FRET measurements. When the G-quadraplex forms, the two fluorophores become close, showing high FRET. A complementary stem strand is used to switch between on and off states. The right panel shows that unfolded state (U) is correlated with low FRET signals, whereas folded states (F_1 and F_2) yield high FRET. Reproduced from [108]. CC BY 3.0.

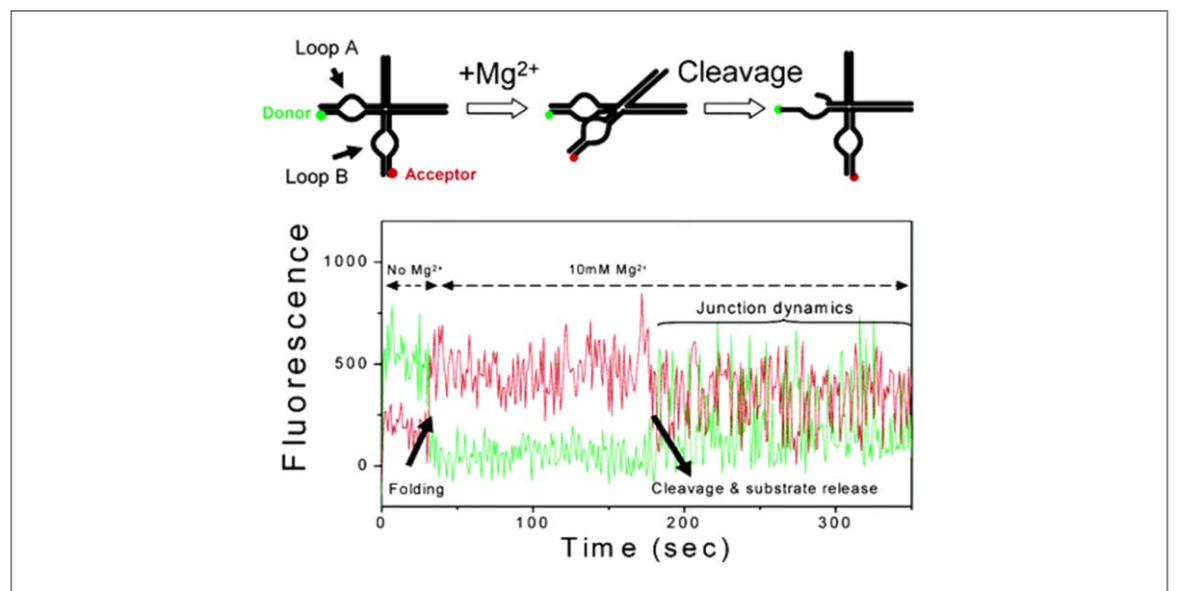


Figure 7. Dynamic conformation change of a hairpin ribozyme. A schematic of detecting folding and catalytic cleavage of the hairpin ribozyme using SM-FRET spectroscopy. The loops A and B will pinch together with Mg^{2+} added which facilitates cleavage of the binding spot. The ribozyme subsequently assumes the open conformation. The corresponding FERT signal changes are shown in the bottom panel. Figure adapted with permission from [113]. Copyright (2004) American Chemical Society.

nanomachines, several strategies have been introduced for such purposes. SM-FRET reveals the kinetics of the rapid transitions between different conformations and helps elucidate how external stimulations affect the changes. Single particle tracking provides time-resolved super-resolution images of moving particles (i.e. fluorophore-labeled DNA) via localization microscopy. Analysis of the trajectories provides information about the translocation dynamics and mechanisms at the nanoscale.

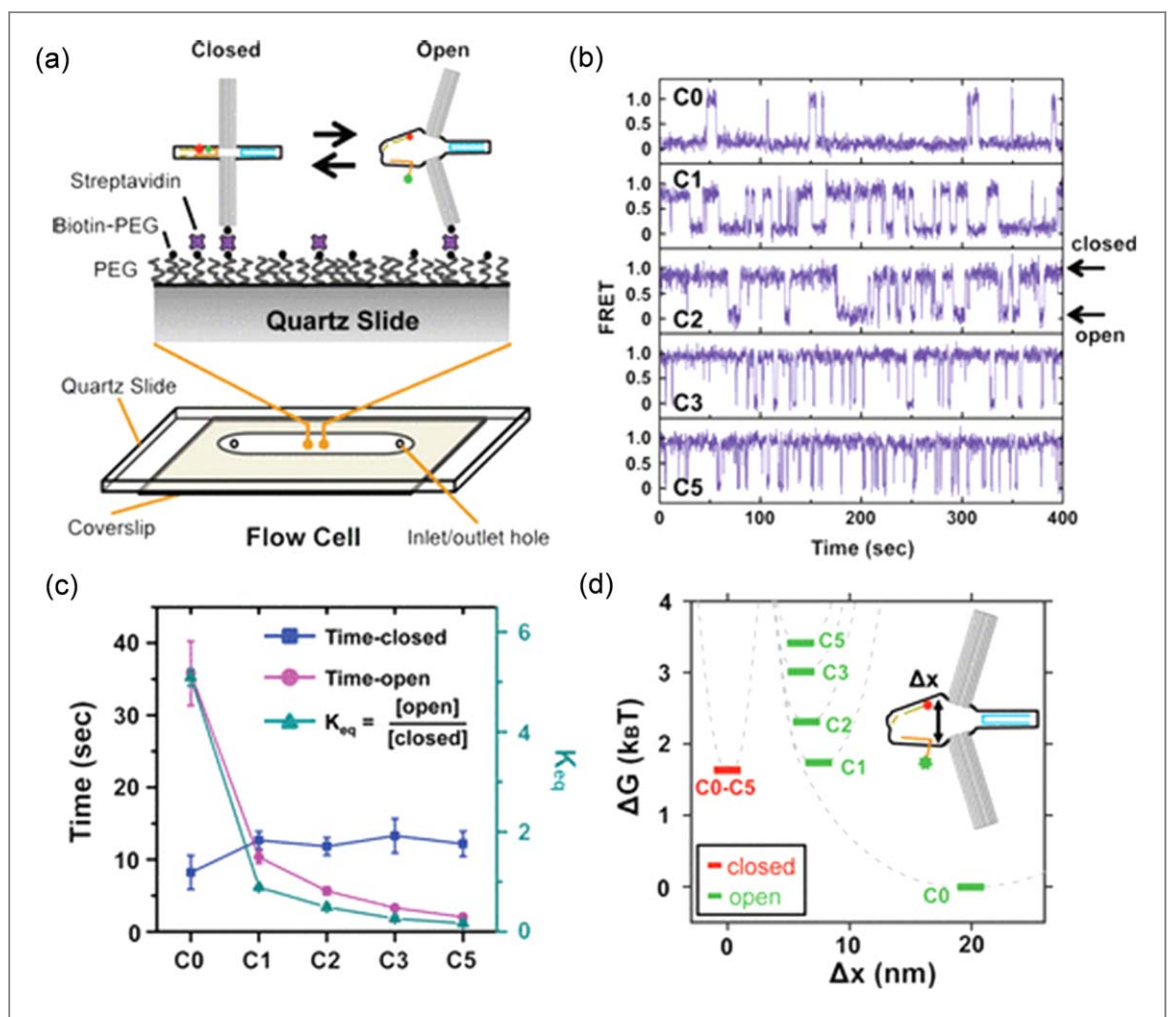


Figure 8. (a) Schematic of closed and open conformations of a DNA origami structure in a flow cell. (b) SM-FRET signal dynamics of the sample with single to multiple constraint linkers. (c) The ratio of dwell time in open to closed states of the sample with different linkers. (d) Free energy landscape corresponding to the distance between the FRET pairs. Figure adapted with permission from [115]. Copyright (2017) American Chemical Society.

3.1. SM-FRET

The advances of SM-FRET spectroscopy enable single molecule detection not only with extreme spatial resolution, but also with high temporal resolution. It has been widely used to investigate subtle conformational changes in DNA nanostructures. Klenerman and colleagues probed the dynamics of a DNA hairpin loop with SM-FRET with a temporal resolution of 20 μ s [112]. The folding and unfolding states of the hairpin loop correspond to high and low FRET signals. Based on the measurements, they analyzed the proximity distribution of different conformations by introducing the mean relaxation time as a key feature in a theoretical a model. The relaxation time was tuned by modulating buffer conditions and the reconfiguration process was controlled by altering the heterogeneity of the system. Ha group investigated the folding and unfolding behaviors of hairpin ribozymes using SM-FRET with temporal resolution of $\sim 10 \,\mu s$ (figure 7) [113, 114]. Analysis of the transition rates between the conformations revealed the shape-changing process where an intermediate structure significantly enhanced the probability to transition to the active

conformation. Castro and co-workers constructed a DNA origami nanodevice which can transform between open and close states as shown in figure 8 [115]. The two states of the structure were correlated with different intensities with SM-FRET signals. From the measurement, they used close versus open time periods and ratio of two energy states to describe the reconfiguration kinetics. They also showed that an addition of polyethylene glycol or PEG can alter the environment of the nanodevice and apply force to change the transformation behaviors. Such controllable behavior could be useful for measuring compressive depletion forces in physical and biological applications [116–119].

3.2. Single particle tracking (SPT)

Recent developments of super-resolution imaging methods allow one to obtain images of single particles/fluorophores with high spatial and temporal resolution. Computer-aided analysis of the images can determine the positions of single particles with standard deviation under 10 nm and show their time-resolved trajectories. Further information such

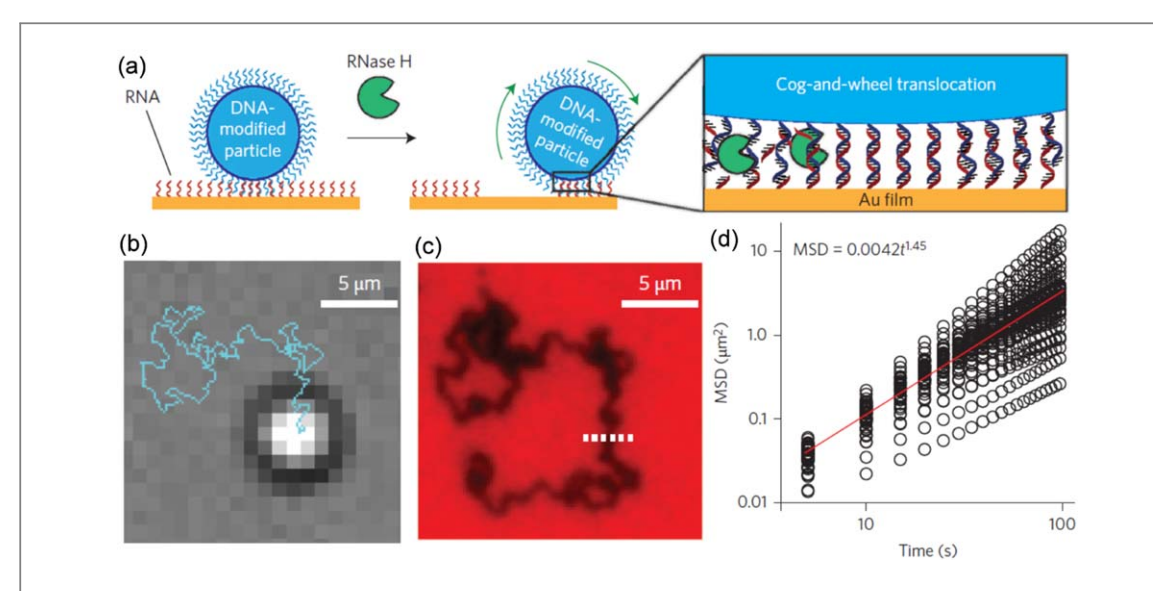


Figure 9. (a) Schematic of particle-modified DNA motors that move on a 2D plane. The particle rolling is powered by RNase H activities on fuel strands on the Au film. Bright-field image (b) and Cy3 fluorescence image. (c) of the single particle trajectory. (d) Mean-squared displacement (MSD) versus time plot reveals self-avoiding mechanisms. Figure adapted from [123] with permission. Copyright © 2016, Springer Nature.

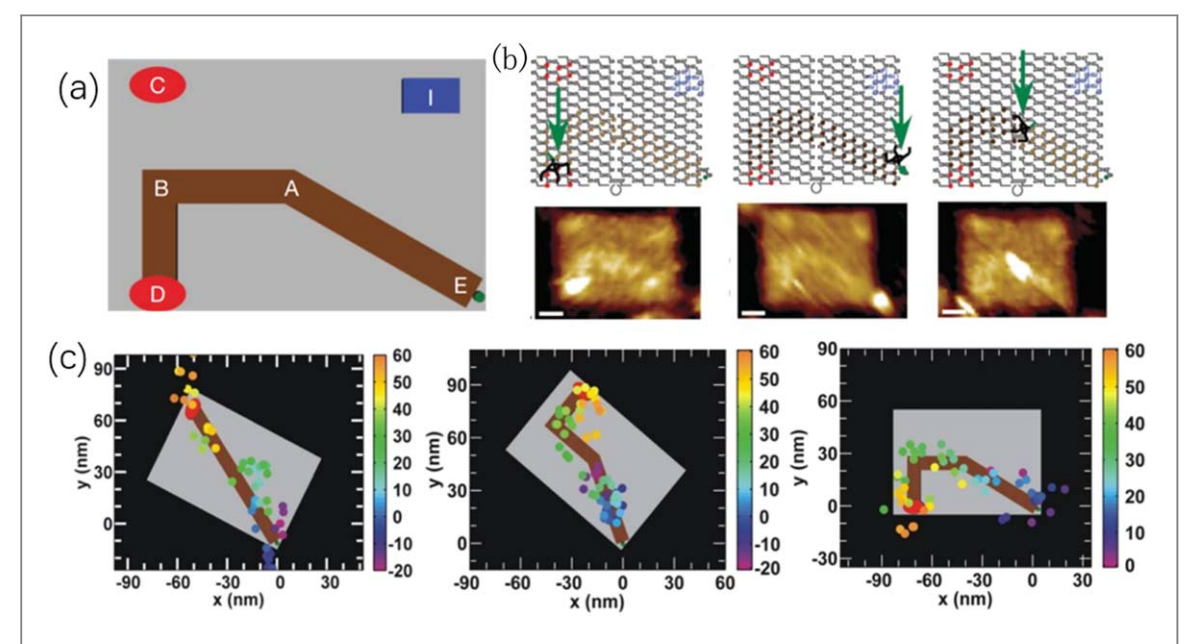


Figure 10. (a) Schematic of the DNA origami track for a multi-legged DNA spider. Here, C is a CONTROL point, I represents a topographical imaging marker. E is the START point, and D represents the STOP point. A and B indicate TURNs. (b) A sequence of spider movement along the track and the corresponding AFM images. (c) Position-time trajectories of selected spiders on the track. The positions as a function of time are represented by color-coded dots. The small green dot in the lower right corner of each track represents the START point, and a large red oval on the other end indicates the STOP point. Figure adapted from [65] with permission. Copyright © 2010, Springer Nature.

as velocity and scaling features may also be obtained [120, 121].

Salome and colleagues used the SPT scheme to monitor the tethered motion of particles immobilized on a surface with DNA [122]. Differential interference contrast (DIC) microscopy was used to monitor the particles with temporal and spatial resolution of 40 ms and 10 nm, respectively. Statistical analysis of multiple particles revealed the effects of the number and length of DNA strands. They found that greater number and

shorter strands result in more restricted motion with smaller maximum displacement Yehl *et al* built a polystyrene particle modified DNA motor that can randomly move on a 2D plane (figure 9) [123]. They used structured illumination microscopy with 110 nm resolution to monitor motor trajectories in real time. Their mean-squared displacement (MSD) analysis showed that the enzyme-powered rolling behavior of the particle-bound DNA motors is based on self-avoiding mechanism.

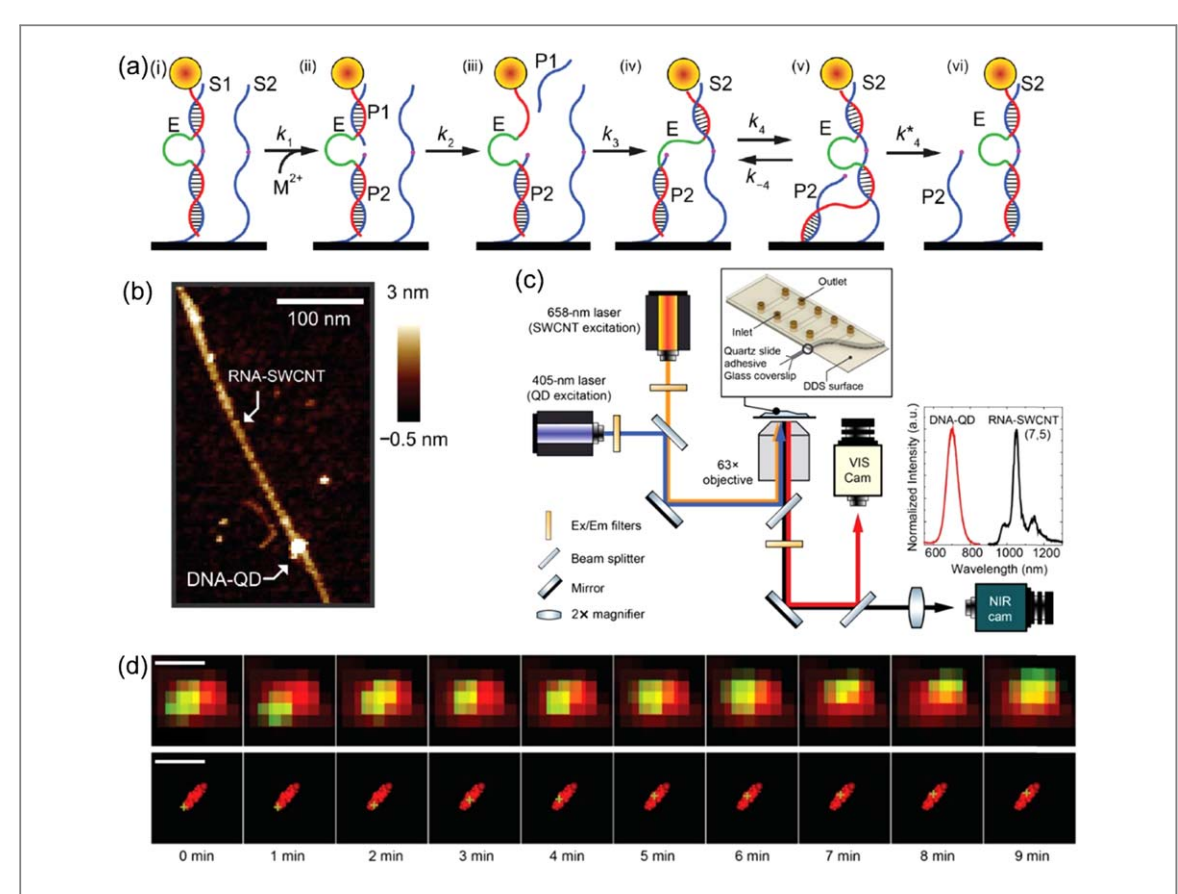


Figure 11. (a) Principle of DNAzyme-based walker that transport QD autonomously, processively along near-infrared-fluorescent carbon nanotube. Inspired by intracellular protein motors, this synthetic molecular motor walks step-by-step through a series of conformational changes. (b) AFM images of QD-modified DNA conjugated with RNA fuel strands decorated on carbon nanotube. (c) Schematic of visible/near-infrared super-resolution fluorescence microscopy using QD and carbon nanotube fluorescence. (d) Raw and subdiffraction images of DNA walker trajectory (green) along immobilized carbon nanotube (red). Figure adapted from [75] with permission. Copyright © 2017, The Authors.

Lund and coworkers demonstrated a multi-legged DNA spider [65] that can carry out a series of autonomous actions including 'start', 'follow', 'turn' and 'stop' in a programmable manner. On a rectangular track from DNA origami (65 nm \times 90 nm \times 2 nm), they marked START, STOP, and Control points as shown in figure 10(a). They used both SPT and AFM for monitoring the motions of the DNA spider. AFM was used to probe the position and estimate the efficiency of spider motion (figure 10(b)). The behaviors of the spider on different tracks were analyzed with or without marked points. SPT-TIRF microscopy monitored real-time movements of the spider (figure 10(c)), yielding a direct comparison between AFM and SPT measurements. It is worth noting that the AFM can monitor multiple spiders at the same time, yet the temporal resolution is relatively low (e.g. of the order of 1 min). The super-resolution SPT is better at monitoring multiple individual spiders with a time resolution of ~10 sec and a spatial resolution of ~ 10 nm.

Choi group demonstrated an autonomous molecular motor that walk step-by-step along a linear track through a series of conformation changes by converting chemical energy into mechanical motion (figure 11). This synthetic walker is reminiscent of intracellular kinesin motor that moves along microtubule. They designed the walker system using a fluorescent quantum dot (QD)-functionalized DNAzyme strand that catalytically cleaves RNA fuel strands decorated on the carbon nanotube with sequence specificity [124]. This walker translocates processively and unidirectionally on the linear track from immobilized carbon nanotubes. They introduced powerful visible/ near-infrared fluorescence microscopy to monitor time-resolved QD trajectories along carbon nanotubes that fluoresce in the second near-infrared spectrum [125]. The visible QD and near-infrared nanotube images from an EMCCD and an InGaAs camera were reconstructed for super-resolved trajectories of DNA walkers with precision of ~20 nm [75]. This novel optical platform revealed the stochastic behavior of single DNA motors. From the new discoveries, they identified the rate-limiting intermediate reactions and provided a set of general design principles for highspeed DNA walkers [77]. As briefly outlined here, the SPT scheme is a powerful platform in probing and analyzing DNA motors and nanomachines, and should also help facilitate other branches of DNA nanotechnology [126, 127].

4. Summary and outlook

With the rapid development of super-resolution fluorescence microscopy, powerful optical imaging platforms are used to study engineered functional DNA nanosystems. Complex nanogeometries and their motion/reconfiguration, as well as reaction dynamics can be probed at single-molecule level, providing critical information about kinetics, mechanics, and energetics.

Despite the rapid development, there are still multiple challenges. For example, 3D imaging is one of them. Most of current super-resolved fluorescence microscopy strategies are applied to acquire 2D images and used from a single perspective at a time, typically from the top view. There are methods to reconstruct images of 3D structures. However, obtaining layer-bylayer images accurately to represent the structure is still a significant challenge, with the accuracy and ranges limited in the z direction compared to 2D x-y planes. Another challenge is combining high spatial resolution with temporal resolution. SPT method has a temporal resolution of the order of a second, while its spatial resolution is roughly 10 nm. A better spatial resolution may be achieved for observing static structures. SM-FRET is capable of probing both static and dynamic single molecules with high temporal and spatial resolutions. However, this method is limited to lengthscale of less than 10 nm and is not suitable for long-range measurements.

Overcoming these challenges will be essential not only to the field of DNA nanotechnology, but also many other areas. Advances of super-resolution microscopy may be used to solve traditionally difficult problems. For example, G-quadruplex has significant implications in biology and medicine, particularly cancer, yet it is difficult to probe the conformation in vivo [128, 129]. Such challenge may benefit from advancement of subdiffraction optical imaging. Similarly, i-motif formation and DNAzyme activities may also be probed [130-134]. In engineering, DNA-based reaction cascades including catalytic hairpin assembly (CHA) and DNA-based nanomachines could also be monitored inside live cells [135–139]. Finally, there are also developing interests in using DNA as scaffolds for nanomanufacturing [140-143]. The ability to probe and evaluate the structures and processes at the single molecule level will continue to grow for years to come. We envision that more advanced, diverse imaging schemes will undoubtedly help establish DNA nanotechnology as foundations for diverse applications.

Acknowledgments

We gratefully acknowledge support from the US Office of Naval Research and National Science Foundation.

ORCID iDs

Jong Hyun Choi https://orcid.org/0000-0002-0507-3052

References

- [1] Watson J D and Crick F H 1953 The structure of DNA, Cold Spring Harbor symposia on quantitative biology (New York: Cold Spring Harbor Laboratory Press) pp 123–31
- [2] Caruthers M H 1985 Gene synthesis machines: DNA chemistry and its uses Science 230 281–5
- [3] Lindahl T 1993 Instability and decay of the primary structure of DNA Nature 362 709–15
- [4] Wolstenholme D R 1992 Animal mitochondrial DNA: structure and evolution. *International Review of cytology* (Amsterdam: Elsevier) Vol. 141, pp 173–216
- [5] Seeman N C 1982 Nucleic acid junctions and lattices *J. Theor. Biol.* **99** 237–47
- [6] Nadrian C S 2003 DNA in a material world Nature 421 427–31
- [7] Tang N, Ma S and Tian J 2013 New tools for cost-effective DNA synthesis In Synthetic Biology (Amsterdam: Elsevier) pp 3–21
- [8] Pinheiro A V, Han D, Shih W M and Yan H 2011 Challenges and opportunities for structural DNA nanotechnology Nat. Nanotechnol. 6763–72
- [9] Carlson R 2009 The changing economics of DNA synthesis Nat. Biotechnol. 27 1091–4
- [10] Seeman N C 1999 DNA engineering and its application to nanotechnology Trend in Biotechnology 17 437–43
- [11] Rangnekar A and LaBean T H 2014 Building DNA Nanostructures for molecular computation, Templated assembly, and Biological Applications Acc. Chem. Res. 47 1778–88
- [12] Kuzuya A and Ohya Y 2014 Nanomechanical molecular devices made of DNA origami Acc. Chem. Res. 47 1742–9
- [13] Douglas S M, Chou J J and Shih W M 2007 DNA-nanotubeinduced alignment of membrane proteins for NMR structure determination *Proc. Natl Acad. Sci. USA* 104 6644—8
- [14] Ke Y, Castro C and Choi J H 2018 Structural DNA nanotechnology: artificial nanostructures for biomedical research Annu. Rev. Biomed. Eng. 20 375–401
- [15] Maune H T, P H S, Barish R D, Bockrath M, Goddard III W A, Rothemund P W K and Winfree E 2009 Self-assembly of carbon nanotubes into two-dimensional geometries using DNA origami templates Nat. Nanotechnol. 5 61–6
- [16] Seelig G, Soloveichik D, Zhang D Y and Winfree E 2006 Enzyme-Free Nucleic Acid Logic Circuits Science 314 1585–8
- [17] Green A A, Silver P A, Collins J J and Yin P 2014 Toehold Switches: De-Novo-Designed Regulators of Gene Expression Cell 159 925–39
- [18] Li F, Chen H, Pan J, Cha T G, Medintz I L and Choi J H 2016 A DNAzyme-mediated logic gate for programming molecular capture and release on DNA origami *Chemical Communications* 52 8369–72
- [19] Wang L.-j., Ren M, Liang L and Zhang C.-y. 2018 Controllable fabrication of bio-bar codes for dendritically amplified sensing of human T-lymphotropic viruses Chemical Science 9 4942–9
- [20] Wang Z.-y., Wang M, Zhang Y and Zhang C.-y. 2018 Sensitive and label-free discrimination of 5-hydroxymethylcytosine and 5-methylcytosine in DNA by ligation-mediated rolling circle amplification *Chemical Communications* 54 8602–5
- [21] Wang L.-j., Han X, Li C.-c. and Zhang C.-y. 2018 Singleribonucleotide repair-mediated ligation-dependent cycling signal amplification for sensitive and specific detection of DNA methyltransferase Chemical science 9 6053–61
- [22] Zhang Y, Li Q.-n., Li C.-c. and Zhang C.-y. 2018 Label-free and high-throughput bioluminescence detection of uracil-DNA

- glycosylase in cancer cells through tricyclic cascade signal amplification *Chemical Communications* **54** 6991–4
- [23] Seeman N C 2010 Nanomaterials based on DNA Annual review of biochemistry 79 65–87
- [24] Rothemund P W 2006 Folding DNA to create nanoscale shapes and patterns *Nature* 440 297–302
- [25] Dietz H, Douglas S M and Shih W M 2009 Folding DNA into twisted and curved nanoscale shapes Science 325 725–30
- [26] Douglas S M, Dietz H, Liedl T, Hogberg B, Graf F and Shih W M 2009 Self-assembly of DNA into nanoscale threedimensional shapes *Nature* 459 414–8
- [27] Shih W M, Quispe J D and Joyce G F 2004 A 1.7-kilobase single-stranded DNA that folds into a nanoscale octahedron *Nature* 427 618–21
- [28] Chen H, Cha T G, Pan J and Choi J H 2013 Hierarchically assembled DNA Origami tubules with reconfigurable chirality Nanotechnology 24 435601
- [29] Chen H, Li F and Choi J H 2014 DNA Origami as programmable nanomanufacturing tools Encyclopedia of Nanotechnology ed B Bhushan (Dordrecht: Springer)
- [30] Chen H, Li R, Li S, Andreasson J and Choi J H 2017 Conformational Effects of UV Light on DNA Origami J. Am. Chem. Soc. 139 1380–3
- [31] Choi J, Chen H, Li F, Yang L, Kim S S, Naik R R, Ye P D and Choi J H 2015 nanomanufacturing of 2D transition metal dichalcogenide materials using self-assembled DNA nanotubes Small 11 5520-7
- [32] Fu Y, Zeng D, Chao J, Jin Y, Zhang Z, Liu H, Li D, Ma H, Huang Q and Gothelf K V 2012 Single-step rapid assembly of DNA origami nanostructures for addressable nanoscale bioreactors J. Am. Chem. Soc. 135 696–702
- [33] Funke J J and Dietz H 2015 Placing molecules with bohr radius resolution using DNA origami Nat. Nanotechnol. 10 47–52
- [34] Jungmann R, Liedl T, Sobey T L, Shih W and Simmel F C 2008 Isothermal assembly of DNA origami structures using denaturing agents J. Am. Chem. Soc. 130 10062–3
- [35] Ke Y, Bellot G, Voigt N V, Fradkov E and Shih W M 2012 Two design strategies for enhancement of multilayer-DNAorigami folding: underwinding for specific intercalator rescue and staple-break positioning *Chemical Science* 3 2587–97
- [36] Li Z, Liu M, Wang L, Nangreave J, Yan H and Liu Y 2010 Molecular behavior of DNA Origami in higher-Order selfassembly J. Am. Chem. Soc. 132 13545–52
- [37] Han D, Pal S, Nangreave J, Deng Z, Liu Y and Yan H 2011 DNA origami with complex curvatures in three-dimensional space Science 332 342–6
- [38] Liu H and Fan C 2013 DNA Origami Nanostructures InDNA Nanotechnology (Berlin: Springer) pp 207–24
- [39] Saccà B and Niemeyer C M 2012 DNA origami: the art of folding DNA Angewandte Chemie International Edition 51 58–66
- [40] Zhang F, Jiang S, Wu S, Li Y, Mao C, Liu Y and Yan H 2015 Complex wireframe DNA origami nanostructures with multi-arm junction vertices Nat. Nanotechnol. 10 779–84
- [41] Chen H, Zhang H, Pan J, Cha T-G, Li S, Andréasson J and Choi J H 2016 Dynamic and progressive control of DNA origami conformation by modulating DNA helicity with chemical adducts ACS Nano 10 4989–96
- [42] Chen H, Weng T-W, Riccitelli M M, Cui Y, Irudayaraj J and Choi J H 2014 Understanding the mechanical properties of DNA origami tiles and controlling the kinetics of their folding and unfolding reconfiguration J. Am. Chem. Soc. 136 6995–7005
- [43] He Y, Ye T, Su M, Zhang C, Ribbe A E and Mao C 2008 Hierarchical self-assembly of DNA into symmetric supramolecular polyhedra *Nature* 452 198–201
- [44] Zhang C, Su M, He Y, Zhao X, Fang P-A, Ribbe A E, Jiang W and Mao C 2008 Conformational flexibility facilitates self-assembly of complex DNA nanostructures *Proc. Natl* Acad. Sci. 105 10665–9
- [45] Ko S H, Su M, Zhang C, Ribbe A E, Jiang W and Mao C 2010 Synergistic self-assembly of RNA and DNA molecules *Nat. Chem.* 2 1050–5

- [46] He Y, Chen Y, Liu H, Ribbe A E and Mao C 2005 Selfassembly of hexagonal DNA two-dimensional (2D) arrays Journal of the American Chemical Soiety 127 12202–3
- [47] He Y, Tian Y, Ribbe A E and Mao C 2006 Antibody nanoarrays with a Pitch of ~20 nanometers *J. Am. Chem. Soc.* 128 12664–5
- [48] Zhang C, He Y, Chen Y, Ribbe A E and Mao C 2007 Aligning One-Dimensional DNA Duplexes into two-dimensional crystals Journal of the American Chemical Soiety 129 14134–5
- [49] Tian C, Li X, Li Z, Jiang W, Wang G and Mao C 2014 Directed Self-Assembly of DNA Tiles into Complex Nanocages Angewandte Chemie 126 8179–82
- [50] Wei B, Dai M and Yin P 2012 Complex Shapes Self-assembled from Single-stranded DNA Tiles Nature 485 623–6
- [51] Ke Y, Ong L L, Shih W M and Yin P 2012 Three-dimensional Structures Self-assembled from DNA Bricks Science 388 1177–83
- [52] Ong L L, Hanikel N, Yaghi O K, Grun C, Strauss M T, Bron P, Lai-Kee-Him J, Schueder F, Wang B and Wang P 2017 Programmable self-assembly of three-dimensional nanostructures from 10,000 unique components *Nature* 552 72–7
- [53] Marras A E, Zhou L, Su H-J and Castro C E 2015 Programmable motion of DNA origami mechanisms *Proc. Natl Acad. Sci.* 112 713–8
- [54] Ketterer P, Willner E M and Dietz H 2016 Nanoscale rotary apparatus formed from tight-fitting 3D DNA components Science Advances 2 e1501209
- [55] Lauback S, Mattioli K R, Marras A E, Armstrong M, Rudibaugh T P, Sooryakumar R and Castro C E 2018 Realtime magnetic actuation of DNA nanodevices via modular integration with stiff micro-levers Nat. Commun. 9 1446
- [56] Yurke B, Turberfield A J, Mills A P Jr, Simmel F C and Neumann J L 2000 A DNA-fuelled molecular machine made of DNA Nature 406 605-8
- [57] Gerling T, Wagenbauer K F, Neuner A M and Dietz H 2015 Dynamic DNA devices and assemblies formed by shapecomplementary, non-base pairing 3D components Science 347 1446–52
- [58] Kuzuya A, Sakai Y, Yamazaki T, Xu Y and Komiyama M 2011 Nanomechanical DNA origami 'single-molecule beacons' directly imaged by atomic force microscopy Nat. Commun. 2 449
- [59] Ke Y, Meyer T, Shih W M and Bellot G 2016 Regulation at a distance of biomolecular interactions using a dna origami nanoactuator Nat. Commun. 7 10935
- [60] Kuzyk A, Urban M J, Idili A, Ricci F and Liu N 2017 Selective control of reconfigurable chiral plasmonic metamolecules *Science Advances* 3 e1602803
- [61] Wickham S F J, Endo M, Katsuda Y, Hidaka K, Bath J, Sugiyama H and Turberfield A J 2011 Direct Observation of Stepwise movement of a synthetic molecular transporter *Nat. Nanotechnol.* 6 166–9
- [62] Bath J, Green S J and Turberfield A J 2005 A Free-Running DNA Motor Powered by a nicking enzyme Angewandte Chemie 44 4358–61
- [63] Yin P, Yan H, Daniell X G, Turberfield A J and Reif J H 2004 A unidirectional DNAwalker that moves autonomously along a track Angewandte Chemie International Edition 43 4906–11
- [64] Gu H, Chao J, Xiao S J and Seeman N C 2010 A Proximitybased Programmable DNA Nanoscale Assembly Line Nature 465 202-5
- [65] Lund K et al 2010 Molecular robots guided by prescriptive landscapes Nature 465 206–10
- [66] Schliwa M and Woehlke G 2001 Switching on Kinesin Nature 411 424–5
- [67] Muthukrishnan G, Hutchins B M, Williams M E and Hancock W O 2006 Transport of semiconductor nanocrystals by kinesin molecular motors Small 2 626–30
- [68] Tsuchiya Y et al 2010 A Polysaccharide-Based Container transportation system powered by molecular motors Angewandte Chemie International Edition 49 724–7

- [69] Laakso J M, Lewis J H, Shuman H and Ostap E M 2008 Myosin I Can Act As a molecular force sensor Science 321 133–6
- [70] Jaeger L and Chworos A 2006 The architectonics of programmable RNA and DNA nanostructures Current opinion in structural biology 16 531–43
- [71] Wilner O I and Willner I 2012 Functionalized DNA nanostructures Chem. Rev. 112 2528–56
- [72] Zhang D Y and Winfree E 2009 Control of DNA strand displacement kinetics using toehold exchange J. Am. Chem. Soc. 131 17303–13
- [73] Zhang D Y and Seelig G 2011 Dynamic DNA nanotechnology using strand displacement reactions Nat. Chem. 3 103–13
- [74] Pan J, Li F, Cha T-G, Chen H and Choi J H 2015 Recent progress on DNA based walkers Current opinion in biotechnology 34 56–64
- [75] Pan J, Cha T-G, Li F, Chen H, Bragg N A and Choi J H 2017 Visible/near-infrared subdiffraction imaging reveals the stochastic nature of DNA walkers Science advances 3 e1601600
- [76] Turberfield A J, Mitchell J, Yurke B, Mills A P Jr, Blakey M and Simmel F C 2003 DNA fuel for free-running nanomachines *Phys. Rev. Lett.* 90 118102
- [77] Cha T-G, Pan J, Chen H, Robinson H N, Li X, Mao C and Choi J H 2015 Design principles of DNA enzyme-based walkers: Translocation kinetics and photoregulation *J. Am. Chem. Soc.* 137 9429–37
- [78] Binnig G, Quate CF and Gerber C 1986 Atomic force microscope Phys. Rev. Lett. 56 930
- [79] Fultz B and Howe J M 2012 Transmission Electron Microscopy And Diffractometry Of Materials. (Berlin: Springer Science & Business Media)
- [80] Scherzer O 1949 The theoretical resolution limit of the electron microscope *J. Appl. Phys.* **20** 20–9
- [81] Sales T R and Morris G M 1997 Fundamental limits of optical superresolution Opt. Lett. 22 582–4
- [82] Borman S and Stevenson R L 1998 Super-resolution from image sequences-a review, Circuits and Systems. Proc. 1998 Midwest Symp. on (Piscataway, NJ) (IEEE) pp 374–8
- [83] Farsiu S, Robinson D, Elad M and Milanfar P 2004 Advances and challenges in super-resolution *Int. J. Imaging Syst. Technol.* 14 47–57
- [84] Huang B, Bates M and Zhuang X 2009 Super-resolution fluorescence microscopy Annual Review Of Biochemistry 78 993–1016
- [85] Park S C, Park M K and Kang M G 2003 Super-resolution image reconstruction: a technical overview *IEEE Signal Process. Mag.* 20 21–36
- [86] Clegg R M 1995 Fluorescence resonance energy transfer Current opinion in Biotechnology 6 103–10
- [87] Ha T, Enderle T, Ogletree D, Chemla D S, Selvin P R and Weiss S 1996 Probing the interaction between two single molecules: fluorescence resonance energy transfer between a single donor and a single acceptor *Proc. Natl Acad. Sci.* 93 6264–8
- [88] Periasamy A 2001 Fluorescence resonance energy transfer microscopy: a mini review J. Biomed. Opt. 6 287–92
- [89] Roy R, Hohng S and Ha T 2008 A practical guide to singlemolecule FRET Nat. Methods 5 507-16
- [90] Willig K I, Rizzoli S O, Westphal V, Jahn R and Hell S W 2006 STED microscopy reveals that synaptotagmin remains clustered after synaptic vesicle exocytosis *Nature* 440 935–9
- [91] Klar T A, Jakobs S, Dyba M, Egner A and Hell S W 2000 Fluorescence microscopy with diffraction resolution barrier broken by stimulated emission *Proc. Natl Acad. Sci.* 97 8206–10
- [92] Müller T, Schumann C and Kraegeloh A 2012 STED microscopy and its applications: new insights into cellular processes on the nanoscale *ChemPhysChem* 13 1986–2000
- [93] Hell S W and Wichmann J 1994 Breaking the diffraction resolution limit by stimulated emission: stimulatedemission-depletion fluorescence microscopy Opt. Lett. 19 780–2

- [94] Jungmann R, Steinhauer C, Scheible M, Kuzyk A, Tinnefeld P and Simmel F C 2010 Single-molecule kinetics and super-resolution microscopy by fluorescence imaging of transient binding on DNA origami Nano Lett. 10 4756–61
- [95] Kim N, Kim H J, Kim Y, Min K S and Kim S K 2016 Direct and precise length measurement of single, stretched DNA fragments by dynamic molecular combing and STED nanoscopy Analytical and bioanalytical chemistry 408 6453–9
- [96] Schoen I, Ries J, Klotzsch E, Ewers H and Vogel V 2011 Binding-activated localization microscopy of DNA structures Nano Lett. 11 4008–11
- [97] Rust M J, Bates M and Zhuang X 2006 Sub-diffraction-limit imaging by stochastic optical reconstruction microscopy (STORM) Nat. Methods 3 793–6
- [98] Huang B, Wang W, Bates M and Zhuang X 2008 Threedimensional super-resolution imaging by stochastic optical reconstruction microscopy *Science* 319 810–3
- [99] Ambrose W P, Goodwin P M and Nolan J P 1999 Single-molecule detection with total internal reflection excitation: Comparing signal-to-background and total signals in different geometries Cytometry: The Journal of the International Society for Analytical Cytology 36 224–31
- [100] Mathur D and Medintz I L 2017 Analyzing DNA nanotechnology: A Call to Arms For The analytical chemistry community Anal. Chem. 89 2646–63
- [101] Steinhauer C, Jungmann R, Sobey T L, Simmel F C and Tinnefeld P 2009 DNA origami as a nanoscopic ruler for super-resolution microscopy Angewandte Chemie International Edition 48 8870–3
- [102] Schmied J Jr, Forthmann C, Pibiri E, Lalkens B, Nickels P, Liedl T and Tinnefeld P 2013 DNA origami nanopillars as standards for three-dimensional superresolution microscopy *Nano Lett.* 13 781–5
- [103] Heller I, Sitters G, Broekmans O D, Farge G, Menges C, Wende W, Hell S W, Peterman E J and Wuite G J 2013 STED nanoscopy combined with optical tweezers reveals protein dynamics on densely covered DNA Nat. Methods 10 910–6
- [104] Jungmann R, Avendano M S, Woehrstein J B, Dai M, Shih W M and Yin P 2014 Multiplexed 3D cellular superresolution Imaging with DNA-PAINT and exchange-PAINT Nat. Methods 11 313–8
- [105] Zhan P, Dutta P K, Wang P, Song G, Dai M, Zhao S-X, Wang Z-G, Yin P, Zhang W and Ding B 2017 Reconfigurable three-dimensional gold nanorod plasmonic nanostructures organized on DNA origami tripod ACS Nano 11 1172–9
- [106] Lin C, Jungmann R, Leifer A M, Li C, Levner D, Church G M, Shih W M and Yin P 2012 Submicrometre geometrically encoded fluorescent barcodes self-assembled from DNA Nat. Chem. 4832–9
- [107] Joo C, McKinney S A, Lilley D M and Ha T 2004 Exploring rare conformational species and ionic effects in DNA holliday junctions using single-molecule spectroscopy *Journal of molecular biology* 341 739–51
- [108] Shirude P S and Balasubramanian S 2008 Single molecule conformational analysis of DNA G-quadruplexes *Biochimie* 90 1197–206
- [109] Woźniak A K, Schröder G F, Grubmüller H, Seidel C A and Oesterhelt F 2008 Single-molecule FRET measures bends and kinks in DNA Proc. Natl Acad. Sci. 105 18337–42
- [110] Saccà B, Ishitsuka Y, Meyer R, Sprengel A, Schöneweiß E C, Nienhaus G U and Niemeyer C M 2015 Reversible reconfiguration of DNA origami nanochambers monitored by single-molecule FRET Angewandte Chemie International Edition 54 3592–7
- [111] Buckhout-White S, Spillmann C M, Algar W R, Khachatrian A, Melinger J S, Goldman E R, Ancona M G and Medintz I L 2014 Assembling programmable FRET-based photonic networks using designer DNA scaffolds Nat. Commun. 5 5615
- [112] Wallace M I, Ying L, Balasubramanian S and Klenerman D 2000 FRET fluctuation spectroscopy: exploring the conformational dynamics of a DNA hairpin loop *The Journal* of *Physical Chemistry* B 104 11551–5

- [113] Ha T 2004 Structural dynamics and processing of nucleic acids revealed by single-molecule spectroscopy *Biochemistry* 43 4055–63
- [114] Tan E, Wilson T J, Nahas M K, Clegg R M, Lilley D M and Ha T 2003 A four-way junction accelerates hairpin ribozyme folding via a discrete intermediate *Proc. Natl Acad. Sci.* 100 9308–13
- [115] Hudoba M W, Luo Y, Zacharias A, Poirier M G and Castro C E 2017 Dynamic DNA Origami device for measuring compressive depletion forces ACS Nano 11 6566–73
- [116] Müller B K, Reuter A, Simmel F C and Lamb D C 2006 Singlepair FRET characterization of DNA tweezers Nano Lett. 6 2814–20
- [117] Xia T, Yuan J and Fang X 2013 Conformational dynamics of an ATP-binding DNA aptamer: a single-molecule study *The Journal of Physical Chemistry* B 117 14994–5003
- [118] Liber M, Tomov T E, Tsukanov R, Berger Y and Nir E 2015 A bipedal DNA motor that travels back and forth between two DNA origami tiles Small 11 568–75
- [119] Ouldridge T E, Hoare R L, Louis A A, Doye J P, Bath J and Turberfield A J 2013 Optimizing DNA nanotechnology through coarse-grained modeling: a two-footed DNA walker ACS Nano 7 2479–90
- [120] Manzo C and Garcia-Parajo M F 2015 A review of progress in single particle tracking: from methods to biophysical insights Rep. Prog. Phys. 78 124601
- [121] Chenouard N, Smal I, De Chaumont F, Maška M, Sbalzarini I F, Gong Y, Cardinale J, Carthel C, Coraluppi S and Winter M 2014 Objective comparison of particle tracking methods *Nat. Methods* 11 281–9
- [122] Pouget N, Dennis C, Turlan C, Grigoriev M, Chandler M and Salomé L 2004 Single-particle tracking for DNA tether length monitoring Nucleic Acids Research 32 e73
- [123] Yehl K, Mugler A, Vivek S, Liu Y, Zhang Y, Fan M, Weeks E R and Salaita K 2016 High-speed DNA-based rolling motors powered by RNase H Nat. Nanotechnol. 11 184–90
- [124] Cha T-G, Pan J, Chen H, Salgado J, Li X, Mao C and Choi J H 2014 A synthetic DNA motor that transports nanoparticles along carbon nanotubes *Nat. Nanotechnol.* 9 39–43
- [125] Pan J, Cha T-G, Chen H, Li F and Choi J H 2017 DNA Walkers as transport vehicles of nanoparticles along a carbon nanotube Track 3D DNA Nanostructure (Berlin: Springer) pp 269–80
- [126] Jung C, Allen P and Ellington A 2016 A stochastic DNA walker that traverses a microparticle surface Nat. Nanotechnol. 11 157–63
- [127] Liang L, Li J, Li Q, Huang Q, Shi J, Yan H and Fan C 2014 Single-particle tracking and modulation of cell entry pathways of a tetrahedral dna nanostructure in live cells Angewandte Chemie International Edition 53 7745–50

- [128] Biffi G, Tannahill D, McCafferty J and Balasubramanian S 2013 Quantitative visualization of DNA G-quadruplex structures in human cells Nat. Chem. 5 182–6
- [129] Han H and Hurley L H 2000 G-quadruplex DNA: a potential target for anti-cancer drug design *Trends in pharmacological* sciences 21 136–42
- [130] Halder S and Krishnan Y 2015 Design of ultrasensitive DNAbased fluorescent pH sensitive nanodevices Nanoscale 7 10008–12
- [131] Leroy J-L, Gueron M, Mergny J-L and Helene C 1994 Intramolecular folding of a fragment of the cytosine-rich strand of telomeric DNA into an i-motif *Nucleic acids research* 22 1600–6
- [132] Li W, Wang J, Ren J and Qu X 2013 Near-infrared-and pHresponsive system for reversible cell adhesion using graphene/gold nanorods functionalized with i-motif DNA Angewandte Chemie 125 6858–62
- [133] Achenbach J, Chiuman W, Cruz R and Li Y 2004 DNAzymes: from creation in vitro to application in vivo Current pharmaceutical biotechnology 5 321–36
- [134] Wu P, Hwang K, Lan T and Lu Y 2013 A DNAzyme-gold nanoparticle probe for uranyl ion in living cells J. Am. Chem. Soc. 135 5254–7
- [135] Jiang Y, Li B, Milligan J N, Bhadra S and Ellington A D 2013 Real-time detection of isothermal amplification reactions with thermostable catalytic hairpin assembly J. Am. Chem. Soc. 135 7430–3
- [136] Zhuang J, Lai W, Chen G and Tang D 2014 A rolling circle amplification-based DNA machine for miRNA screening coupling catalytic hairpin assembly with DNAzyme formation Chemical communications 50 2935–8
- [137] Li F, Cha T G, Pan J, Ozcelikkale A, Han B and Choi J H 2016 DNA Walker-Regulated Cancer Cell growth inhibition ChemBioChem 17 1138–41
- [138] Walsh A S, Yin H, Erben C M, Wood M J and Turberfield A J 2011 DNA cage delivery to mammalian cells ACS Nano 5 5427–32
- [139] Modi S, Swetha M, Goswami D, Gupta G D, Mayor S and Krishnan Y 2009 A DNA nanomachine that maps spatial and temporal pH changes inside living cells Nat. Nanotechnol. 4 325–30
- [140] Mastroianni A J, Claridge S A and Alivisatos A P 2009 Pyramidal and chiral groupings of gold nanocrystals assembled using DNA scaffolds J. Am. Chem. Soc. 131 8455–9
- [141] Perez J M, O'Loughin T, Simeone F J, Weissleder R and Josephson L 2002 DNA-based magnetic nanoparticle assembly acts as a magnetic relaxation nanoswitch allowing screening of DNA-cleaving agents J. Am. Chem. Soc. 124 2856–7
- [142] Mirkin C A, Letsinger R L, Mucic R C and Storhoff J J 1996 A DNA-based method for rationally assembling nanoparticles into macroscopic materials *Nature* 382 607–9
- [143] Simmel F C 2012 DNA-based assembly lines and nanofactories Current Opinion in Biotechnology 23 516–21